

Precise Measurement of the χ_{c0} Resonance Parameters and Branching Fractions of

$$\chi_{c0,c2} \rightarrow \pi^+\pi^-/K^+K^-$$

M. Ablikim¹, M. N. Achasov^{4,c}, P. Adlarson⁷⁶, O. Afedulidis³, X. C. Ai⁸¹, R. Aliberti³⁵, A. Amoroso^{75A,75C}, Y. Bai⁵⁷, O. Bakina³⁶, I. Balossino^{29A}, Y. Ban^{46,h}, H.-R. Bao⁶⁴, V. Batozskaya^{1,44}, K. Begzsuren³², N. Berger³⁵, M. Berlowski⁴⁴, M. Bertani^{28A}, D. Bettoni^{29A}, F. Bianchi^{75A,75C}, E. Bianco^{75A,75C}, A. Bortone^{75A,75C}, I. Boyko³⁶, R. A. Briere⁵, A. Brueggemann⁶⁹, H. Cai⁷⁷, X. Cai^{1,58}, A. Calcaterra^{28A}, G. F. Cao^{1,64}, N. Cao^{1,64}, S. A. Cetin^{62A}, X. Y. Chai^{46,h}, J. F. Chang^{1,58}, G. R. Che⁴³, Y. Z. Che^{1,58,64}, G. Chelkov^{36,b}, C. Chen⁴³, C. H. Chen⁹, Chao Chen⁵⁵, G. Chen¹, H. S. Chen^{1,64}, H. Y. Chen²⁰, M. L. Chen^{1,58,64}, S. J. Chen⁴², S. L. Chen⁴⁵, S. M. Chen⁶¹, T. Chen^{1,64}, X. R. Chen^{31,64}, X. T. Chen^{1,64}, Y. B. Chen^{1,58}, Y. Q. Chen³⁴, Z. J. Chen^{25,i}, Z. Y. Chen^{1,64}, S. K. Choi¹⁰, G. Cibinetto^{29A}, F. Cossio^{75C}, J. J. Cui⁵⁰, H. L. Dai^{1,58}, J. P. Dai⁷⁹, A. Dbeysy¹⁸, R. E. de Boer³, D. Dedovich³⁶, C. Q. Deng⁷³, Z. Y. Deng¹, A. Denig³⁵, I. Denysenko³⁶, M. Destefanis^{75A,75C}, F. De Mori^{75A,75C}, B. Ding^{67,1}, X. X. Ding^{46,h}, Y. Ding⁴⁰, Y. Ding³⁴, J. Dong^{1,58}, L. Y. Dong^{1,64}, M. Y. Dong^{1,58,64}, X. Dong⁷⁷, M. C. Du¹, S. X. Du⁸¹, Y. Y. Duan⁵⁵, Z. H. Duan⁴², P. Egorov^{36,b}, Y. H. Fan⁴⁵, J. Fang^{1,58}, J. Fang⁵⁹, S. S. Fang^{1,64}, W. X. Fang¹, Y. Fang¹, Y. Q. Fang^{1,58}, R. Farinelli^{29A}, L. Fava^{75B,75C}, F. Feldbauer³, G. Felici^{28A}, C. Q. Feng^{72,58}, J. H. Feng⁵⁹, Y. T. Feng^{72,58}, M. Fritsch³, C. D. Fu¹, J. L. Fu⁶⁴, Y. W. Fu^{1,64}, H. Gao⁶⁴, X. B. Gao⁴¹, Y. N. Gao^{46,h}, Yang Gao^{72,58}, S. Garbolino^{75C}, I. Garzia^{29A,29B}, L. Ge⁸¹, P. T. Ge¹⁹, Z. W. Ge⁴², C. Geng⁵⁹, E. M. Gersabeck⁶⁸, A. Gilman⁷⁰, K. Goetzen¹³, L. Gong⁴⁰, W. X. Gong^{1,58}, W. Grad³⁵, S. Gramigna^{29A,29B}, M. Greco^{75A,75C}, M. H. Gu^{1,58}, Y. T. Gu¹⁵, C. Y. Guan^{1,64}, A. Q. Guo^{31,64}, L. B. Guo⁴¹, M. J. Guo⁵⁰, R. P. Guo⁴⁹, Y. P. Guo^{12,g}, A. Guskov^{36,b}, J. Gutierrez²⁷, K. L. Han⁶⁴, T. T. Han¹, F. Hanisch³, X. Q. Hao¹⁹, F. A. Harris⁶⁶, K. K. He⁵⁵, K. L. He^{1,64}, F. H. Heinsius³, C. H. Heinz³⁵, Y. K. Heng^{1,58,64}, C. Herold⁶⁰, T. Holtmann³, P. C. Hong³⁴, G. Y. Hou^{1,64}, X. T. Hou^{1,64}, Y. R. Hou⁶⁴, Z. L. Hou¹, B. Y. Hu⁵⁹, H. M. Hu^{1,64}, J. F. Hu^{56,j}, Q. P. Hu^{72,58}, S. L. Hu^{12,g}, T. Hu^{1,58,64}, Y. Hu¹, G. S. Huang^{72,58}, K. X. Huang⁵⁹, L. Q. Huang^{31,64}, X. T. Huang⁵⁰, Y. P. Huang¹, Y. S. Huang⁵⁹, T. Hussain⁷⁴, F. Hölzken³, N. Hüsken³⁵, N. in der Wiesche⁶⁹, J. Jackson²⁷, S. Janchiv³², J. H. Jeong¹⁰, Q. Ji¹, Q. P. Ji¹⁹, W. Ji^{1,64}, X. B. Ji^{1,64}, X. L. Ji^{1,58}, Y. Y. Ji⁵⁰, X. Q. Jia⁵⁰, Z. K. Jia^{72,58}, D. Jiang^{1,64}, H. B. Jiang⁷⁷, P. C. Jiang^{46,h}, S. S. Jiang³⁹, T. J. Jiang¹⁶, X. S. Jiang^{1,58,64}, Y. Jiang⁶⁴, X. B. Jiao⁵⁰, J. K. Jiao³⁴, Z. Jiao²³, S. Jin⁴², Y. Jin⁶⁷, M. Q. Jing^{1,64}, X. M. Jing⁶⁴, T. Johansson⁷⁶, S. Kabana³³, N. Kalantar-Nayestanaki⁶⁵, X. L. Kang⁹, X. S. Kang⁴⁰, M. Kavatsyuk⁶⁵, B. C. Ke⁸¹, V. Khachatryan²⁷, A. Khokkaz⁶⁹, R. Kiuchi¹, O. B. Kolcu^{62A}, B. Kopf³, M. Kuessner³, X. Kui^{1,64}, N. Kumar²⁶, A. Kupsc^{44,76}, W. Kühn³⁷, L. Lavezzi^{75A,75C}, T. T. Lei^{72,58}, Z. H. Lei^{72,58}, M. Lellmann³⁵, T. Lenz³⁵, C. Li⁴³, C. Li⁴⁷, C. H. Li³⁹, Cheng Li^{72,58}, D. M. Li⁸¹, F. Li^{1,58}, G. Li¹, H. B. Li^{1,64}, H. J. Li¹⁹, H. N. Li^{56,j}, Hui Li⁴³, J. R. Li⁶¹, J. S. Li⁵⁹, K. Li¹, K. L. Li¹⁹, L. J. Li^{1,64}, L. K. Li¹, Lei Li⁴⁸, M. H. Li⁴³, P. R. Li^{38,k,l}, Q. M. Li^{1,64}, Q. X. Li⁵⁰, R. Li^{17,31}, S. X. Li¹², T. Li⁵⁰, T. Y. Li⁴³, W. D. Li^{1,64}, W. G. Li^{1,a}, X. Li^{1,64}, X. H. Li^{72,58}, X. L. Li⁵⁰, X. Y. Li^{1,8}, X. Z. Li⁵⁹, Y. G. Li^{46,h}, Z. J. Li⁵⁹, Z. Y. Li⁷⁹, C. Liang⁴², H. Liang^{72,58}, H. Liang^{1,64}, Y. F. Liang⁵⁴, Y. T. Liang^{31,64}, G. R. Liao¹⁴, Y. P. Liao^{1,64}, J. Libby²⁶, A. Limphirat⁶⁰, C. C. Lin⁵⁵, C. X. Lin⁶⁴, D. X. Lin^{31,64}, T. Lin¹, B. J. Liu¹, B. X. Liu⁷⁷, C. Liu³⁴, C. X. Liu¹, F. Liu¹, F. H. Liu⁵³, Feng Liu⁶, G. M. Liu^{56,j}, H. Liu^{38,k,l}, H. B. Liu¹⁵, H. H. Liu¹, H. M. Liu^{1,64}, Huihui Liu²¹, J. B. Liu^{72,58}, J. Y. Liu^{1,64}, K. Liu^{38,k,l}, K. Y. Liu⁴⁰, Ke Liu²², L. Liu^{72,58}, L. C. Liu⁴³, Lu Liu⁴³, M. H. Liu^{12,g}, P. L. Liu¹, Q. Liu⁶⁴, S. B. Liu^{72,58}, T. Liu^{12,g}, W. K. Liu⁴³, W. M. Liu^{72,58}, X. Liu^{38,k,l}, X. Liu³⁹, Y. Liu⁸¹, Y. Liu^{38,k,l}, Y. B. Liu⁴³, Z. A. Liu^{1,58,64}, Z. D. Liu⁹, Z. Q. Liu⁵⁰, X. C. Lou^{1,58,64}, F. X. Lu⁵⁹, H. J. Lu²³, J. G. Lu^{1,58}, X. L. Lu¹, Y. Lu⁷, Y. P. Lu^{1,58}, Z. H. Lu^{1,64}, C. L. Luo⁴¹, J. R. Luo⁵⁹, M. X. Luo⁸⁰, T. Luo^{12,g}, X. L. Luo^{1,58}, X. R. Lyu⁶⁴, Y. F. Lyu⁴³, F. C. Ma⁴⁰, H. Ma⁷⁹, H. L. Ma¹, J. L. Ma^{1,64}, L. L. Ma⁵⁰, L. R. Ma⁶⁷, M. M. Ma^{1,64}, Q. M. Ma¹, R. Q. Ma^{1,64}, T. Ma^{72,58}, X. T. Ma^{1,64}, X. Y. Ma^{1,58}, Y. M. Ma³¹, F. E. Maas¹⁸, I. MacKay⁷⁰, M. Maggiora^{75A,75C}, S. Malde⁷⁰, Y. J. Mao^{46,h}, Z. P. Mao¹, S. Marcello^{75A,75C}, Z. X. Meng⁶⁷, J. G. Messchendorp^{13,65}, G. Mezzadri^{29A}, H. Miao^{1,64}, T. J. Min⁴², R. E. Mitchell²⁷, X. H. Mo^{1,58,64}, B. Moses²⁷, N. Yu. Muchnoi^{4,c}, J. Muskalla³⁵, Y. Nefedov³⁶, F. Nerling^{18,e}, L. S. Nie²⁰, I. B. Nikolaev^{4,c}, Z. Ning^{1,58}, S. Nisar^{11,m}, Q. L. Niu^{38,k,l}, W. D. Niu⁵⁵, Y. Niu⁵⁰, S. L. Olsen⁶⁴, S. L. Olsen^{10,64}, Q. Ouyang^{1,58,64}, S. Pacetti^{28B,28C}, X. Pan⁵⁵, Y. Pan⁵⁷, A. Pathak³⁴, Y. P. Pei^{72,58}, M. Pelizaeus³, H. P. Peng^{72,58}, Y. Y. Peng^{38,k,l}, K. Peters^{13,e}, J. L. Ping⁴¹, R. G. Ping^{1,64}, S. Plura³⁵, V. Prasad³³, F. Z. Qi¹, H. Qi^{72,58}, H. R. Qi⁶¹, M. Qi⁴², T. Y. Qi^{12,g}, S. Qian^{1,58}, W. B. Qian⁶⁴, C. F. Qiao⁶⁴, X. K. Qiao⁸¹, J. J. Qin⁷³, L. Q. Qin¹⁴, L. Y. Qin^{72,58}, X. P. Qin^{12,g}, X. S. Qin⁵⁰, Z. H. Qin^{1,58}, J. F. Qiu¹, Z. H. Qu⁷³, C. F. Redmer³⁵, K. J. Ren³⁹, A. Rivetti^{75C}, M. Rolo^{75C}, G. Rong^{1,64}, Ch. Rosner¹⁸, M. Q. Ruan^{1,58}, S. N. Ruan⁴³, N. Salone⁴⁴, A. Sarantsev^{36,d}, Y. Schelhaas³⁵, K. Schoenning⁷⁶, M. Scodreggio^{29A}, K. Y. Shan^{12,g}, W. Shan²⁴, X. Y. Shan^{72,58}, Z. J. Shang^{38,k,l}, J. F. Shangguan¹⁶, L. G. Shao^{1,64}, M. Shao^{72,58}, C. P. Shen^{12,g}, H. F. Shen^{1,8}, W. H. Shen⁶⁴, X. Y. Shen^{1,64}, B. A. Shi⁶⁴, H. Shi^{72,58}, J. L. Shi^{12,g}, J. Y. Shi¹, Q. Q. Shi⁵⁵, S. Y. Shi⁷³, X. Shi^{1,58}, J. J. Song¹⁹, T. Z. Song⁵⁹, W. M. Song^{34,1}, Y. J. Song^{12,g}, Y. X. Song^{46,h,n}, S. Sosio^{75A,75C}, S. Spataro^{75A,75C}, F. Stiele³⁵, S. S. Su⁴⁰, Y. J. Su⁶⁴, G. B. Sun⁷⁷, G. X. Sun¹, H. Sun⁶⁴, H. K. Sun¹, J. F. Sun¹⁹, K. Sun⁶¹, L. Sun⁷⁷, S. S. Sun^{1,64}, T. Sun^{51,f}, W. Y. Sun³⁴, Y. Sun⁹, Y. J. Sun^{72,58}, Y. Z. Sun¹, Z. Q. Sun^{1,64}, Z. T. Sun⁵⁰, C. J. Tang⁵⁴, G. Y. Tang¹, J. Tang⁵⁹, M. Tang^{72,58}, Y. A. Tang⁷⁷, L. Y. Tao⁷³, Q. T. Tao^{25,i}, M. Tat⁷⁰, J. X. Teng^{72,58}, V. Thoren⁷⁶, W. H. Tian⁵⁹, Y. Tian^{31,64}, Z. F. Tian⁷⁷, I. Uman^{62B}, Y. Wan⁵⁵, S. J. Wang⁵⁰, B. Wang¹, B. L. Wang⁶⁴, Bo Wang^{72,58}, D. Y. Wang^{46,h}, F. Wang⁷³, H. J. Wang^{38,k,l}, J. J. Wang⁷⁷, J. P. Wang⁵⁰, K. Wang^{1,58}, L. L. Wang¹, M. Wang⁵⁰, N. Y. Wang⁶⁴, S. Wang^{12,g}, S. Wang^{38,k,l}, T. Wang^{12,g}, T. J. Wang⁴³, W. Wang⁵⁹, W. Wang⁷³, W. P. Wang^{35,58,72,o}, X. Wang^{46,h}, X. F. Wang^{38,k,l}, X. J. Wang³⁹, X. L. Wang^{12,g}, X. N. Wang¹, Y. Wang⁶¹, Y. D. Wang⁴⁵, Y. F. Wang^{1,58,64}, Y. H. Wang^{38,k,l}, Y. L. Wang¹⁹, Y. N. Wang⁴⁵, Y. Q. Wang¹, Yaqian Wang¹⁷, Yi Wang⁶¹, Z. Wang^{1,58}, Z. L. Wang⁷³, Z. Y. Wang^{1,64}, Ziyi Wang⁶⁴, D. H. Wei¹⁴, F. Weidner⁶⁹, S. P. Wen¹, Y. R. Wen³⁹, U. Wiedner³, G. Wilkinson⁷⁰, M. Wolke⁷⁶, L. Wollenberg³, C. Wu³⁹, J. F. Wu^{1,8}, L. H. Wu¹, L. J. Wu^{1,64}, X. Wu^{12,g}, X. H. Wu³⁴, Y. Wu^{72,58}, Y. H. Wu⁵⁵, Y. J. Wu³¹, Z. Wu^{1,58}, L. Xia^{72,58}, X. M. Xian³⁹, B. H. Xiang^{1,64}, T. Xiang^{46,h}, D. Xiao^{38,k,l}, G. Y. Xiao⁴², S. Y. Xiao¹, Y. L. Xiao^{12,g}, Z. J. Xiao⁴¹, C. Xie⁴², X. H. Xie^{46,h}, Y. Xie⁵⁰, Y. G. Xie^{1,58}, Y. H. Xie⁶, Z. P. Xie^{72,58}, T. Y. Xing^{1,64}, C. F. Xu^{1,64}, C. J. Xu⁵⁹, G. F. Xu¹, H. Y. Xu^{67,2}, M. Xu^{72,58}, Q. J. Xu¹⁶, Q. N. Xu³⁰, W. Xu¹, W. L. Xu⁶⁷, X. P. Xu⁵⁵, Y. Xu⁴⁰, Y. C. Xu⁷⁸, Z. S. Xu⁶⁴, F. Yan^{12,g}, L. Yan^{12,g}, W. B. Yan^{72,58}, W. C. Yan⁸¹, X. Q. Yan^{1,64}, H. J. Yang^{51,f}, H. L. Yang³⁴, H. X. Yang¹, J. H. Yang⁴², T. Yang¹, Y. Yang^{12,g}, Y. F. Yang^{1,64}, Y. F. Yang⁴³, Y. X. Yang^{1,64}, Z. W. Yang^{38,k,l}, Z. P. Yao⁵⁰, M. Ye^{1,58}, M. H. Ye⁸, J. H. Yin¹, Junhao Yin⁴³, Z. Y. You⁵⁹, B. X. Yu^{1,58,64}, C. X. Yu⁴³, G. Yu^{1,64}, J. S. Yu^{25,i}, M. C. Yu⁴⁰, T. Yu⁷³, X. D. Yu^{46,h}, Y. C. Yu⁸¹, C. Z. Yuan^{1,64}, J. Yuan⁴⁵, J. Yuan³⁴, L. Yuan², S. C. Yuan^{1,64}, Y. Yuan^{1,64}, Z. Y. Yuan⁵⁹, C. X. Yue³⁹, A. A. Zafar⁷⁴, F. R. Zeng⁵⁰, S. H. Zeng^{63A,63B,63C,63D}, X. Zeng^{12,g}, Y. Zeng^{25,i}

Y. J. Zeng^{1,64}, Y. J. Zeng⁵⁹, X. Y. Zhai³⁴, Y. C. Zhai⁵⁰, Y. H. Zhan⁵⁹, A. Q. Zhang^{1,64}, B. L. Zhang^{1,64}, B. X. Zhang¹, D. H. Zhang⁴³, G. Y. Zhang¹⁹, H. Zhang⁸¹, H. Zhang^{72,58}, H. C. Zhang^{1,58,64}, H. H. Zhang³⁴, H. H. Zhang⁵⁹, H. Q. Zhang^{1,58,64}, H. R. Zhang^{72,58}, H. Y. Zhang^{1,58}, J. Zhang⁸¹, J. Zhang⁵⁹, J. J. Zhang⁵², J. L. Zhang²⁰, J. Q. Zhang⁴¹, J. S. Zhang^{12,g}, J. W. Zhang^{1,58,64}, J. X. Zhang^{38,k,l}, J. Y. Zhang¹, J. Z. Zhang^{1,64}, Jianyu Zhang⁶⁴, L. M. Zhang⁶¹, Lei Zhang⁴², P. Zhang^{1,64}, Q. Y. Zhang³⁴, R. Y. Zhang^{38,k,l}, S. H. Zhang^{1,64}, Shulei Zhang^{25,i}, X. M. Zhang¹, X. Y. Zhang⁴⁰, X. Y. Zhang⁵⁰, Y. Zhang¹, Y. Zhang⁷³, Y. T. Zhang⁸¹, Y. H. Zhang^{1,58}, Y. M. Zhang³⁹, Yan Zhang^{72,58}, Z. D. Zhang¹, Z. H. Zhang¹, Z. L. Zhang³⁴, Z. Y. Zhang⁴³, Z. Y. Zhang⁷⁷, Z. Z. Zhang⁴⁵, G. Zhao¹, J. Y. Zhao^{1,64}, J. Z. Zhao^{1,58}, L. Zhao¹, Lei Zhao^{72,58}, M. G. Zhao⁴³, N. Zhao⁷⁹, R. P. Zhao⁶⁴, S. J. Zhao⁸¹, Y. B. Zhao^{1,58}, Y. X. Zhao^{31,64}, Z. G. Zhao^{72,58}, A. Zhemchugov^{36,b}, B. Zheng⁷³, B. M. Zheng³⁴, J. P. Zheng^{1,58}, W. J. Zheng^{1,64}, Y. H. Zheng⁶⁴, B. Zhong⁴¹, X. Zhong⁵⁹, H. Zhou⁵⁰, J. Y. Zhou³⁴, L. P. Zhou^{1,64}, S. Zhou⁶, X. Zhou⁷⁷, X. K. Zhou⁶, X. R. Zhou^{72,58}, X. Y. Zhou³⁹, Y. Z. Zhou^{12,g}, Z. C. Zhou²⁰, A. N. Zhu⁶⁴, J. Zhu⁴³, K. Zhu¹, K. J. Zhu^{1,58,64}, K. S. Zhu^{12,g}, L. Zhu³⁴, L. X. Zhu⁶⁴, S. H. Zhu⁷¹, T. J. Zhu^{12,g}, W. D. Zhu⁴¹, Y. C. Zhu^{72,58}, Z. A. Zhu^{1,64}, J. H. Zou¹, J. Zu^{72,58}

(BESIII Collaboration)

¹ Institute of High Energy Physics, Beijing 100049, People's Republic of China

² Beihang University, Beijing 100191, People's Republic of China

³ Bochum Ruhr-University, D-44780 Bochum, Germany

⁴ Budker Institute of Nuclear Physics SB RAS (BINP), Novosibirsk 630090, Russia

⁵ Carnegie Mellon University, Pittsburgh, Pennsylvania 15213, USA

⁶ Central China Normal University, Wuhan 430079, People's Republic of China

⁷ Central South University, Changsha 410083, People's Republic of China

⁸ China Center of Advanced Science and Technology, Beijing 100190, People's Republic of China

⁹ China University of Geosciences, Wuhan 430074, People's Republic of China

¹⁰ Chung-Ang University, Seoul, 06974, Republic of Korea

¹¹ COMSATS University Islamabad, Lahore Campus, Defence Road, Off Raiwind Road, 54000 Lahore, Pakistan

¹² Fudan University, Shanghai 200433, People's Republic of China

¹³ GSI Helmholtzcentre for Heavy Ion Research GmbH, D-64291 Darmstadt, Germany

¹⁴ Guangxi Normal University, Guilin 541004, People's Republic of China

¹⁵ Guangxi University, Nanning 530004, People's Republic of China

¹⁶ Hangzhou Normal University, Hangzhou 310036, People's Republic of China

¹⁷ Hebei University, Baoding 071002, People's Republic of China

¹⁸ Helmholtz Institute Mainz, Staudinger Weg 18, D-55099 Mainz, Germany

¹⁹ Henan Normal University, Xinxiang 453007, People's Republic of China

²⁰ Henan University, Kaifeng 475004, People's Republic of China

²¹ Henan University of Science and Technology, Luoyang 471003, People's Republic of China

²² Henan University of Technology, Zhengzhou 450001, People's Republic of China

²³ Huangshan College, Huangshan 245000, People's Republic of China

²⁴ Hunan Normal University, Changsha 410081, People's Republic of China

²⁵ Hunan University, Changsha 410082, People's Republic of China

²⁶ Indian Institute of Technology Madras, Chennai 600036, India

²⁷ Indiana University, Bloomington, Indiana 47405, USA

²⁸ INFN Laboratori Nazionali di Frascati, (A)INFN Laboratori Nazionali di Frascati, I-00044, Frascati, Italy; (B)INFN Sezione di Perugia, I-06100, Perugia, Italy; (C)University of Perugia, I-06100, Perugia, Italy

²⁹ INFN Sezione di Ferrara, (A)INFN Sezione di Ferrara, I-44122, Ferrara, Italy; (B)University of Ferrara, I-44122, Ferrara, Italy

³⁰ Inner Mongolia University, Hohhot 010021, People's Republic of China

³¹ Institute of Modern Physics, Lanzhou 730000, People's Republic of China

³² Institute of Physics and Technology, Peace Avenue 54B, Ulaanbaatar 13330, Mongolia

³³ Instituto de Alta Investigación, Universidad de Tarapacá, Casilla 7D, Arica 1000000, Chile

³⁴ Jilin University, Changchun 130012, People's Republic of China

³⁵ Johannes Gutenberg University of Mainz, Johann-Joachim-Becher-Weg 45, D-55099 Mainz, Germany

³⁶ Joint Institute for Nuclear Research, 141980 Dubna, Moscow region, Russia

³⁷ Justus-Liebig-Universitaet Giessen, II. Physikalisches Institut, Heinrich-Buff-Ring 16, D-35392 Giessen, Germany

³⁸ Lanzhou University, Lanzhou 730000, People's Republic of China

³⁹ Liaoning Normal University, Dalian 116029, People's Republic of China

⁴⁰ Liaoning University, Shenyang 110036, People's Republic of China

⁴¹ Nanjing Normal University, Nanjing 210023, People's Republic of China

⁴² Nanjing University, Nanjing 210093, People's Republic of China

⁴³ Nankai University, Tianjin 300071, People's Republic of China

⁴⁴ National Centre for Nuclear Research, Warsaw 02-093, Poland

⁴⁵ North China Electric Power University, Beijing 102206, People's Republic of China

⁴⁶ Peking University, Beijing 100871, People's Republic of China

⁴⁷ Qufu Normal University, Qufu 273165, People's Republic of China

⁴⁸ Renmin University of China, Beijing 100872, People's Republic of China

⁴⁹ Shandong Normal University, Jinan 250014, People's Republic of China

- ⁵⁰ Shandong University, Jinan 250100, People's Republic of China
- ⁵¹ Shanghai Jiao Tong University, Shanghai 200240, People's Republic of China
- ⁵² Shanxi Normal University, Linfen 041004, People's Republic of China
- ⁵³ Shanxi University, Taiyuan 030006, People's Republic of China
- ⁵⁴ Sichuan University, Chengdu 610064, People's Republic of China
- ⁵⁵ Soochow University, Suzhou 215006, People's Republic of China
- ⁵⁶ South China Normal University, Guangzhou 510006, People's Republic of China
- ⁵⁷ Southeast University, Nanjing 211100, People's Republic of China
- ⁵⁸ State Key Laboratory of Particle Detection and Electronics, Beijing 100049, Hefei 230026, People's Republic of China
- ⁵⁹ Sun Yat-Sen University, Guangzhou 510275, People's Republic of China
- ⁶⁰ Suranaree University of Technology, University Avenue 111, Nakhon Ratchasima 30000, Thailand
- ⁶¹ Tsinghua University, Beijing 100084, People's Republic of China
- ⁶² Turkish Accelerator Center Particle Factory Group, (A)Istinye University, 34010, Istanbul, Turkey; (B)Near East University, Nicosia, North Cyprus, 99138, Mersin 10, Turkey
- ⁶³ University of Bristol, (A)H H Wills Physics Laboratory; (B)Tyndall Avenue; (C)Bristol; (D)BS8 8TL
- ⁶⁴ University of Chinese Academy of Sciences, Beijing 100049, People's Republic of China
- ⁶⁵ University of Groningen, NL-9747 AA Groningen, The Netherlands
- ⁶⁶ University of Hawaii, Honolulu, Hawaii 96822, USA
- ⁶⁷ University of Jinan, Jinan 250022, People's Republic of China
- ⁶⁸ University of Manchester, Oxford Road, Manchester, M13 9PL, United Kingdom
- ⁶⁹ University of Muenster, Wilhelm-Klemm-Strasse 9, 48149 Muenster, Germany
- ⁷⁰ University of Oxford, Keble Road, Oxford OX13RH, United Kingdom
- ⁷¹ University of Science and Technology Liaoning, Anshan 114051, People's Republic of China
- ⁷² University of Science and Technology of China, Hefei 230026, People's Republic of China
- ⁷³ University of South China, Hengyang 421001, People's Republic of China
- ⁷⁴ University of the Punjab, Lahore-54590, Pakistan
- ⁷⁵ University of Turin and INFN, (A)University of Turin, I-10125, Turin, Italy; (B)University of Eastern Piedmont, I-15121, Alessandria, Italy; (C)INFN, I-10125, Turin, Italy
- ⁷⁶ Uppsala University, Box 516, SE-75120 Uppsala, Sweden
- ⁷⁷ Wuhan University, Wuhan 430072, People's Republic of China
- ⁷⁸ Yantai University, Yantai 264005, People's Republic of China
- ⁷⁹ Yunnan University, Kunming 650500, People's Republic of China
- ⁸⁰ Zhejiang University, Hangzhou 310027, People's Republic of China
- ⁸¹ Zhengzhou University, Zhengzhou 450001, People's Republic of China
- ^a Deceased
- ^b Also at the Moscow Institute of Physics and Technology, Moscow 141700, Russia
- ^c Also at the Novosibirsk State University, Novosibirsk, 630090, Russia
- ^d Also at the NRC "Kurchatov Institute", PNPI, 188300, Gatchina, Russia
- ^e Also at Goethe University Frankfurt, 60323 Frankfurt am Main, Germany
- ^f Also at Key Laboratory for Particle Physics, Astrophysics and Cosmology, Ministry of Education; Shanghai Key Laboratory for Particle Physics and Cosmology; Institute of Nuclear and Particle Physics, Shanghai 200240, People's Republic of China
- ^g Also at Key Laboratory of Nuclear Physics and Ion-beam Application (MOE) and Institute of Modern Physics, Fudan University, Shanghai 200443, People's Republic of China
- ^h Also at State Key Laboratory of Nuclear Physics and Technology, Peking University, Beijing 100871, People's Republic of China
- ⁱ Also at School of Physics and Electronics, Hunan University, Changsha 410082, China
- ^j Also at Guangdong Provincial Key Laboratory of Nuclear Science, Institute of Quantum Matter, South China Normal University, Guangzhou 510006, China
- ^k Also at MOE Frontiers Science Center for Rare Isotopes, Lanzhou University, Lanzhou 730000, People's Republic of China
- ^l Also at Lanzhou Center for Theoretical Physics, Lanzhou University, Lanzhou 730000, People's Republic of China
- ^m Also at the Department of Mathematical Sciences, IBA, Karachi 75270, Pakistan
- ⁿ Also at Ecole Polytechnique Federale de Lausanne (EPFL), CH-1015 Lausanne, Switzerland
- ^o Also at Helmholtz Institute Mainz, Staudinger Weg 18, D-55099 Mainz, Germany

(Dated: February 14, 2025)

By analyzing a $\psi(3686)$ data sample containing $(107.7 \pm 0.6) \times 10^6$ events taken with the BESIII detector at the BEPCII storage ring in 2009, the χ_{c0} resonance parameters are precisely measured using $\chi_{c0,e2} \rightarrow \pi^+\pi^-/K^+K^-$ events. The mass of χ_{c0} is determined to be $M(\chi_{c0}) = (3415.67 \pm 0.07 \pm 0.06 \pm 0.07) \text{ MeV}/c^2$, and its full width is $\Gamma(\chi_{c0}) = (12.44 \pm 0.12 \pm 0.12) \text{ MeV}$, where the first uncertainty is statistical, the second systematic, and the third for mass comes from χ_{c2} mass uncertainty. These measurements improve the precision of χ_{c0} mass by a factor of four and width by one order of magnitude over the previous individual measurements, and significantly boost our knowledge about the charmonium spectrum. Together with additional $(345.4 \pm 2.6) \times 10^6$ $\psi(3686)$ data events taken in 2012, the decay branching fractions of $\chi_{c0,e2} \rightarrow \pi^+\pi^-/K^+K^-$ are measured as well, with precision improved by a factor of three compared to previous measurements. These χ_{c0}

decay branching fractions provide important inputs for the study of glueballs.

PACS numbers:

Charmonium, the bound state of charm and anti-charm quarks governed by the strong force, is analogous to the ‘hydrogen atom’ in the study of meson spectroscopy [1, 2]. Due to its heavy mass, the velocity of the charm quark is relative slow and therefore the system can be well described by a non-relativistic potential model [3]. By now, the charmonium spectroscopy below the open-charm threshold is well established [4], and a precise study of them is important and necessary for a stringent test of the theory of the strong interaction, quantum chromodynamics (QCD). The χ_{cJ} ($J = 0, 1, 2$) charmonia are P -wave $c\bar{c}$ states split by spin-orbit and tensor forces. At the moment, the χ_{c1} and χ_{c2} masses are precisely measured using a scan approach with $p\bar{p}$ annihilation by the E760 [5] and E835 [6] experiments, and by the LHCb [7] experiment in pp collisions, whereas a precise χ_{c0} mass measurement is relatively marginal, with an uncertainty about five times larger [8, 9] than that of $\chi_{c1,c2}$. Improved precision on the χ_{c0} mass is important for probing the spin structure of the strong force, such as the fine structure splitting $M(^3P_2) - M(^3P_0)$, and the singlet-triplet splitting $M(^1P_1) - M_{\text{cog}}(^3P_J)$, where $M_{\text{cog}}(^3P_J)$ is the center-of-gravity of the triplet. This helps precisely determine the spin-orbit and tensor forces.

We also lack knowledge about the precise width of χ_{c0} [4] compared to its $J = 1, 2$ partners [5–7]. A precise width measurement of χ_{c0} serves as an essential input for studying the χ_{c0} decay, such as the $E1$ transition partial width, light hadron decay width, etc. Furthermore, lattice QCD calculation shows an excited scalar glueball candidate with mass in the range of 2.8 – 3.7 GeV [10–12], and the χ_{c0} might contain a gluonic admixture due to the presence of such a nearby glueball. In this sense, the precise χ_{c0} width provides valuable knowledge to investigate excited glueball spectrum, which was used to explain the $\gamma^* \rightarrow (c\bar{c})(c\bar{c})$ cross section discrepancy [13] between perturbative QCD calculations [14, 15] and the experimental measurement [16].

The decay of χ_{c0} to light hadrons proceeds predominately via two-gluon exchanges (color-singlet) [17]. For the simplest pseudo-scalar final state $\pi^+\pi^-$ and K^+K^- , the decay widths are expected to be identical within SU(3) flavor symmetry. This simple feature also applies to other 0^{++} system, such as a light glueball candidate $f_0(1500)/f_0(1710)$ [4]. However, the couplings of $f_0(1710)$ to $\pi^+\pi^-$ and K^+K^- final states differ significantly [18, 19] due to a so-called ‘Chiral Suppression’ effect [20, 21]. Therefore, a precise measurement of the branching fraction (BF) $\chi_{c0} \rightarrow \pi^+\pi^-/K^+K^-$, together with its full width, provides an ideal test ground for the study of decays of the glueball candidates. In addition, the color-octet component also plays an important role in charmonium decays, and these precise BF measurements can help constrain the non-perturbative parameters in QCD calculations [17, 22]

and finally understand the decay dynamics of charmonium states.

In this Letter, a precise mass and width measurement of χ_{c0} is achieved via the $\chi_{c0} \rightarrow \pi^+\pi^-/K^+K^-$ decays. The decay BFs of $\chi_{c0,c2} \rightarrow \pi^+\pi^-/K^+K^-$ are precisely measured as well. The analysis is performed based on a $\psi(3686)$ data sample consisting of $(107.7 \pm 0.6) \times 10^6$ events taken in 2009 and $(345.4 \pm 2.6) \times 10^6$ events taken in 2012 [23] at BESIII. The $\chi_{c0,c2}$ states are produced copiously in the radiative transition $\psi(3686) \rightarrow \gamma\chi_{c0,c2}$.

The BESIII detector [24] records symmetric e^+e^- collisions provided by the BEPCII storage ring [25] in the center-of-mass energy range from 1.85 to 4.95 GeV, with a peak luminosity of $1.1 \times 10^{33} \text{ cm}^{-2}\text{s}^{-1}$ achieved at $\sqrt{s} = 3.773 \text{ GeV}$. BESIII has collected large data samples in this energy region [26]. The cylindrical core of the BESIII detector covers 93% of the full solid angle and consists of a helium-based multilayer drift chamber (MDC), a plastic scintillator time-of-flight system (TOF), and a CsI(Tl) electromagnetic calorimeter (EMC), which are all enclosed in a superconducting solenoidal magnet providing a 1.0 T magnetic field. The solenoid is supported by an octagonal flux-return yoke with resistive plate counter muon identification modules interleaved with steel. The charged-particle momentum resolution at 1 GeV/c is 0.5%, and the resolution of the specific ionization energy loss dE/dx is 6% for electrons from Bhabha scattering. The EMC measures photon energies with a resolution of 2.5% (5%) at 1 GeV in the barrel (end-cap) region. The time resolution in the TOF barrel region is 68 ps, while that in the end-cap region is 110 ps.

Simulated Monte Carlo (MC) samples produced with a GEANT4-based [27] MC simulation software package, which includes the geometric description of the detector and the detector response, are used to determine detection efficiencies, optimize the selection criteria, and estimate background contributions. Signal MC samples of $\psi(3686) \rightarrow \gamma\chi_{c0,c2} \rightarrow \gamma\pi^+\pi^-/\gamma K^+K^-$ are produced. Each channel contains 400,000 signal events. In the simulation, the $\psi(3686)$ resonance is generated with KKMC [28, 29], with beam energy spread and initial-state-radiation effect considered. The decays of $\psi(3686) \rightarrow \gamma\chi_{c0,c2} \rightarrow \gamma\pi^+\pi^-/\gamma K^+K^-$ are simulated with the angular distribution taken into account, using a previous multipole amplitude measurement by BESIII [30].

To investigate the potential background, an inclusive MC sample containing the same number of $\psi(3686)$ events as data is simulated. The inclusive MC sample includes the production of the $\psi(3686)$ resonance, the ISR production of the J/ψ , and the continuum processes incorporated in KKMC [28, 29]. All particle decays are modeled with EVTGEN [31, 32] using BFs either taken from the Particle Data Group (PDG) [4], when available, or otherwise modeled with

LUNDCHARM [33, 34] for remaining unknown charmonium decays. Final state radiation (FSR) from charged final state particles is incorporated using the PHOTOS package [35]. Di-muon and Bhabha MC samples, each containing one million events are generated with the Babayaga generator [36] for further background studies.

For the $\psi(3686) \rightarrow \gamma\chi_{c0,c2} \rightarrow \gamma\pi^+\pi^-/\gamma K^+K^-$ signal events of interest, the final states have two high-momentum charged tracks and an energetic radiative photon [with an energy of 261 (128) MeV in the χ_{c0} (χ_{c2}) case] due to the large mass gap between $\psi(3686)$ and $\chi_{c0,c2}$. Charged tracks detected in the MDC are required to be within a polar angle (θ) range of $|\cos\theta| < 0.93$, where θ is defined with respect to the z axis, which is the symmetry axis of the MDC. For each good charged track, the distance of closest approach to the interaction point (IP) must be less than 10 cm along the z axis, and less than 1 cm in the transverse plane. A candidate event is required to have two good charged tracks with zero net charge.

Photon candidates are identified using isolated showers in the EMC. The deposited energy of each shower must be more than 25 MeV in the barrel region ($|\cos\theta| < 0.80$) and more than 50 MeV in the end-cap region ($0.86 < |\cos\theta| < 0.92$). To exclude showers that originate from charged tracks, the angle subtended by the EMC shower and the position of the closest charged track at the EMC must be greater than 10 degrees as measured from the IP. To suppress electronic noise and showers unrelated to the event, the difference between the EMC time and the event start time is required to be within [0, 700] ns. At least one good photon candidate is required in an event.

To improve the momentum resolution of final state particles and further suppress background, a four-constraint (4C) kinematic fit which constrains the four-momentum of two charged tracks and a photon to the initial $\psi(3686)$ four-momentum is performed. The two charged tracks are assumed to be pairs of $\pi^+\pi^-$ and K^+K^- , respectively, and the corresponding kinematic fit chi-squares ($\chi_{\gamma\pi^+\pi^-}^2$ and $\chi_{\gamma K^+K^-}^2$) are obtained. An event is assigned as $\gamma\pi^+\pi^-$ if $\chi_{\gamma\pi^+\pi^-}^2 < \chi_{\gamma K^+K^-}^2$, otherwise as γK^+K^- . The radiative photon candidate is selected as the one that yields the smallest χ^2 from the 4C kinematic fit if there are multiple photon candidates within one event. The χ^2 of the kinematic fit is further required to be less than 60 for $\gamma\pi^+\pi^-$ events and 56 for γK^+K^- events, which are optimized by maximizing the Figure-of-Merit $S/\sqrt{(S+B)}$, where S represents the number of normalized events from signal MC samples according to BFs from the PDG [4], and B is the total number of normalized background events estimated from the inclusive MC sample, Bhabha and di-muon MC samples.

For $\gamma\pi^+\pi^-$ events, there are radiative Bhabha and $\psi(3686) \rightarrow (\gamma)e^+e^-$ backgrounds. To remove these electrons, the deposited energy of each charged track in the EMC is required to be less than 1.34 GeV. Due to the EMC gap ($0.81 < |\cos\theta| < 0.86$) without crystals between the barrel and end-cap regions, electrons passing the gap can further

survive. To remove these remaining electrons, the dE/dx of a charged particle measured by the MDC is used. For charged tracks falling into the gap region, the $|\chi_{dE/dx}(\pi)|$ [24] is required to be less than 2, where $\chi_{dE/dx}(\pi)$ is the pull value of dE/dx based on the pion hypothesis. The most significant background comes from radiative di-muon and $\psi(3686) \rightarrow (\gamma)\mu^+\mu^-$ events due to serious π and μ mis-identification. These non-peaking background processes are precisely known [4], and can be well simulated at BESIII.

For γK^+K^- events, the background level is much lower due to the higher kaon mass than pion. There are some remaining background from radiative Bhabha, $\psi(3686) \rightarrow (\gamma)e^+e^-$, and $\psi(3686) \rightarrow \pi^0\pi^0 J/\psi \rightarrow \pi^0\pi^0 e^+e^-$. They are effectively vetoed by requiring the deposited energy of both kaons in the EMC to be less than 1.34 GeV. Since no particle identification is applied to high momentum pions and kaons, there is cross-contamination between $\gamma\pi^+\pi^-$ and γK^+K^- events. According to MC simulation studies, the cross-contamination ratio is small ($< 1\%$). For γK^+K^- events, the background contribution from $\gamma\pi^+\pi^-$ cross-contamination is fixed via MC simulation, and vice versa.

After applying the event selection criteria mentioned above, the obtained $M(\pi^+\pi^-)$ and $M(K^+K^-)$ invariant mass distributions from data are shown in Fig. 1, where significant numbers of $\chi_{c0,c2}$ signal events are observed. To measure the mass, and width of χ_{c0} as well as the BFs of $\chi_{c0,c2} \rightarrow \pi^+\pi^-/K^+K^-$, an unbinned maximum likelihood fit is performed to the $\gamma\pi^+\pi^-$ and γK^+K^- data events simultaneously. In the fit, the BFs of $\chi_{c0,c2} \rightarrow \pi^+\pi^-$ and $\chi_{c0,c2} \rightarrow K^+K^-$ are shared as common parameters between data taken in different years. To avoid the absolute mass scale and therefore significantly improve the mass precision of χ_{c0} , the mass split between χ_{c2} and χ_{c0} , *i.e.* $\Delta M_{20} \equiv M(\chi_{c2}) - M(\chi_{c0})$, is measured instead. Even in this case, the quality of the 2012 data is not as good as the 2009 data due to the worse MDC inner chamber performances during data taking [37], which bring in considerable systematic effects from discrepancies between data and MC simulation. Therefore, only the 2009 data are used for mass and width measurements, *i.e.* ΔM_{20} and the full width Γ of χ_{c0} are shared as common parameters in $\gamma\pi^+\pi^-$ and γK^+K^- data events taken in 2009.

The signal probability-density-function (PDF) is parameterized as

$$[\text{BW}^2(\sqrt{s}) \times \mathcal{P}\mathcal{S}_1^2(\sqrt{s}) \times \mathcal{D}^2(\sqrt{s}) \times \mathcal{P}\mathcal{S}_2^2(\chi_{c0,c2} \rightarrow \pi^+\pi^-/K^+K^-) \times \epsilon(\sqrt{s})] \otimes \text{Resolution}, \quad (1)$$

where $\text{BW}(\sqrt{s})$ is a relativistic Breit-Wigner (BW) amplitude defined as

$$\text{BW}(\sqrt{s}) = \frac{1}{s - M^2 + iM\Gamma}, \quad (2)$$

with \sqrt{s} , M and Γ as the $\pi^+\pi^-/K^+K^-$ invariant mass, mass and width of $\chi_{c0,c2}$, respectively. In the $E1$ radiative transition $\psi(3686) \rightarrow \gamma\chi_{c0,c2}$, the decay width is proportional to a

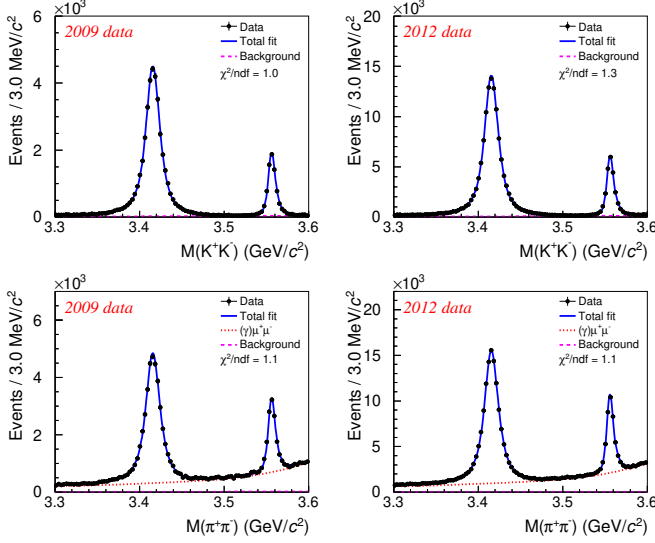


FIG. 1. The K^+K^- (top row) and $\pi^+\pi^-$ (bottom row) invariant mass distributions from $\psi(3686)$ data taken in 2009 (first column) and 2012 (second column) with fit results overlaid. The black dots with error bars are data, the blue solid curves represent the total fit results, the red dotted lines in bottom panels represent the background component from $(\gamma)\mu^+\mu^-$, and the pink dashed lines represent all other background components.

phase space factor $\mathcal{PS}_1(\sqrt{s})$ [38, 39] defined as

$$\mathcal{PS}_1(\sqrt{s}) = \left(\frac{E_\gamma}{E_\gamma^0}\right)^{3/2}, \quad (3)$$

where E_γ is the radiative photon energy and E_γ^0 corresponds to the photon energy at the $\chi_{c0,c2}$ mass M . An additional damping factor $\mathcal{D}(\sqrt{s}) = \left(\frac{(E_\gamma^0)^2}{E_\gamma^0 E_\gamma + (E_\gamma^0 - E_\gamma)^2}\right)^{1/2}$ [40] is also introduced to suppress the higher energy tail. $\mathcal{PS}_2(\chi_{c0,c2} \rightarrow \pi^+\pi^-/K^+K^-)$ is the phase space factor of $\chi_{c0,c2}$ decaying into $\pi^+\pi^-/K^+K^-$ [4]. The signal PDF is corrected by a mass dependent efficiency curve $\epsilon(\sqrt{s})$, which is obtained by MC simulation studies and varies within 1% for the interested mass region, thus parameterized as a linear function. The $\chi_{c0,c2}$ resonance line shapes are further convolved with Gaussian functions to account for the detector resolution. In the fit, the χ_{c2} width are fixed to the known values [4], and the resolution difference between data and MC simulation measured from χ_{c2} data events are used to calibrate that for χ_{c0} .

The shapes of dominant background sources are described by polynomial functions. For γK^+K^- events, the background is low and parameterized as a free second-order polynomial. The small cross-contamination contribution from $\gamma\pi^+\pi^-$ events is fixed via MC simulation. For $\gamma\pi^+\pi^-$ events, the dominated $(\gamma)\mu^+\mu^-$ background is represented by a fourth-order polynomial, which is fixed according to normalized MC events for $\psi(3686) \rightarrow (\gamma)\mu^+\mu^-$ and di-muon processes. Other extra backgrounds with a small contribution

($\sim 3\%$ of the total background) are parameterized as a free second-order polynomial.

Figure 1 shows the fit results. The mass split between χ_{c2} and χ_{c0} is measured to be $\Delta M_{20} \equiv M(\chi_{c2}) - M(\chi_{c0}) = (140.50 \pm 0.07) \text{ MeV}/c^2$. Taking the world average mass $M(\chi_{c2}) = (3556.17 \pm 0.07) \text{ MeV}/c^2$ [4] as input, the χ_{c0} mass is calculated to be $M(\chi_{c0}) = (3415.67 \pm 0.07) \text{ MeV}/c^2$. The width of χ_{c0} is measured to be $\Gamma(\chi_{c0}) = (12.44 \pm 0.12) \text{ MeV}$. The uncertainties here are statistical only.

The systematic uncertainties in the mass split and χ_{c0} width measurements mainly come from signal shape, damping factor, background shapes, and possible mass dependent scale. In the nominal fit model, a BW function with a constant width, *i.e.* Eq. 2, is used to describe the χ_{c0} state. An alternative shape with a mass dependent BW function is investigated. The full width of χ_{c0} is taken as $\Gamma(\sqrt{s}) = \Gamma_0\left(\frac{p}{p'}\right)\left(\frac{M}{\sqrt{s}}\right)$, where Γ_0 is the constant width and p (p') is the momentum of daughter particles in the rest frame of the mother particle with mass \sqrt{s} (M). The difference with respect to the nominal measurement for ΔM_{20} is $0.04 \text{ MeV}/c^2$ and for the χ_{c0} full width $\Gamma(\chi_{c0})$ is 0.10 MeV , which are taken as systematic uncertainties. A damping factor also appears in the signal PDF. We take another form $\mathcal{D}(\sqrt{s}) = e^{-E_\gamma^2/(8\beta^2)}$, where $\beta = 65.0 \pm 2.5 \text{ MeV}$ from the CLEO-c Collaboration [41]. The difference on the measurements of ΔM_{20} is $0.01 \text{ MeV}/c^2$ and $\Gamma(\chi_{c0})$ is 0.01 MeV .

The uncertainty due to background in the fit is studied in several aspects. The free background components are described by second-order polynomials for both $\gamma\pi^+\pi^-$ and γK^+K^- events. Changing this component to a third-order polynomial either for $\gamma\pi^+\pi^-$ or for γK^+K^- events yields differences on the measurements, which are $0.02 \text{ MeV}/c^2$ for ΔM_{20} and 0.04 MeV for $\Gamma(\chi_{c0})$. For $\gamma\pi^+\pi^-$ events, the dominant background comes from $(\gamma)\mu^+\mu^-$. Varying the output cross section from Babayaga [36] by $\pm 1\sigma$ for MC simulated background normalization yields a difference of $0.02 \text{ MeV}/c^2$ for ΔM_{20} and 0.02 MeV for $\Gamma(\chi_{c0})$. The shape parameters of this background component are also varied within $\pm 1\sigma$, which yields a difference of $0.01 \text{ MeV}/c^2$ for ΔM_{20} and 0.02 MeV for $\Gamma(\chi_{c0})$. The possible mass dependent scale is simulated by MC. The systematic uncertainty due to difference between data and MC simulation is studied by correcting the MC distribution to data, which yields a variation of $0.03 \text{ MeV}/c^2$ for ΔM_{20} and 0.01 MeV for $\Gamma(\chi_{c0})$.

Table I summarizes all these sources and their corresponding contributions. Assuming all the sources are independent, the total systematic uncertainty is obtained by adding each individual source in quadrature, which is $0.06 \text{ MeV}/c^2$ for ΔM_{20} and 0.12 MeV for $\Gamma(\chi_{c0})$.

The BF of $\chi_{c0,c2} \rightarrow \pi^+\pi^-/K^+K^-$ is calculated as

$$\mathcal{B} = \frac{N_{\text{sig}}}{N_{\text{tot}}[\psi(3686)]\epsilon\mathcal{B}[\psi(3686) \rightarrow \gamma\chi_{c0,c2}]}, \quad (4)$$

where N_{sig} is the number of observed $\chi_{c0,c2}$ signal events from the fit, $N_{\text{tot}}[\psi(3686)]$ is the total number of col-

TABLE I. Sources of systematic uncertainties and their contributions to ΔM_{20} and $\Gamma(\chi_{c0})$ measurements.

Source	ΔM_{20} (MeV/c ²)	$\Gamma(\chi_{c0})$ (MeV)
Signal shape	0.04	0.10
Damping factor	0.01	0.01
Polynomial background	0.02	0.04
Number of $(\gamma)\mu^+\mu^-$ background	0.02	0.02
Shape of $(\gamma)\mu^+\mu^-$ background	0.01	0.02
Mass dependent scale	0.03	0.01
Total	0.06	0.12

lected $\psi(3686)$ events [23], ϵ is the detection efficiency of $\gamma\pi^+\pi^-/\gamma K^+K^-$ events, and $\mathcal{B}[\psi(3686) \rightarrow \gamma\chi_{c0,c2}]$ is the BF of the $E1$ radiative transition [4]. In practice, a simultaneous fit is performed and the BFs are shared between different data sets. The BFs are measured to be $\mathcal{B}(\chi_{c0} \rightarrow K^+K^-) = (6.36 \pm 0.02) \times 10^{-3}$, $\mathcal{B}(\chi_{c0} \rightarrow \pi^+\pi^-) = (6.06 \pm 0.02) \times 10^{-3}$, $\mathcal{B}(\chi_{c2} \rightarrow K^+K^-) = (1.22 \pm 0.01) \times 10^{-3}$, and $\mathcal{B}(\chi_{c2} \rightarrow \pi^+\pi^-) = (1.61 \pm 0.01) \times 10^{-3}$, respectively, where all the uncertainties are statistical only. Table II lists the detection efficiencies for each data set.

TABLE II. The detection efficiencies for $\gamma\pi^+\pi^-$ and γK^+K^- data events taken in different years.

	$\epsilon(\gamma\pi^+\pi^-)$	$\epsilon(\gamma K^+K^-)$
2009 χ_{c0}	0.644 ± 0.001	0.589 ± 0.001
2009 χ_{c2}	0.667 ± 0.001	0.624 ± 0.001
2012 χ_{c0}	0.634 ± 0.001	0.577 ± 0.001
2012 χ_{c2}	0.658 ± 0.001	0.613 ± 0.001

The systematic uncertainties in the BF measurements mainly come from the total number of $\psi(3686)$ events, detection efficiencies, signal shape, background shapes, fit range, 4C kinematic fit, and intermediate BFs.

The total number of $\psi(3686)$ events is measured by counting inclusive hadronic events, with an uncertainty of 0.7% [23]. Detection efficiencies include tracking, photon detection, decay angular distributions, and selection criteria. The uncertainty of photon detection is measured to be 0.5% per photon by studying the $e^+e^- \rightarrow \gamma\mu^+\mu^-$ process and 0.5% is assigned for this analysis. Pion and kaon tracks have a momentum above 1 GeV. The tracking efficiency of such a track is $> 99\%$ at BESIII, by studying $e^+e^- \rightarrow \pi^+\pi^-\pi^+\pi^-$ and $J/\psi \rightarrow K^*K$ events. According to the two-dimensional (2D, p_t vs. $\cos\theta$) tracking efficiencies of data and MC simulation, the uncertainty in each bin is obtained. The final uncertainty due to tracking is estimated as a weighted average over 2D bins.

Decay angular distributions also affect the detection efficiencies. Considering the helicity amplitudes and correlation coefficients measured by BESIII [30], 100 sets of two cor-

related helicity amplitude parameters are obtained via a 2D sampling. The resulting changes in detection efficiencies and therefore corresponding change of BFs from the simultaneous fit are taken as systematic uncertainty. The uncertainties due to pion/kaon EMC deposit energy requirement and fit range are studied via a Barlow test [42], by changing a series of EMC deposit energies and fit ranges. All the alternative choices give results within 1σ of the nominal result, which means these two sources can be ignored.

For 4C kinematic fit, a correction of pull distribution of charged track parameters is applied to MC simulation [43]. The uncertainties are taken as half of the efficiency difference with or without helix parameter corrections. The uncertainties on the BFs for $\psi(3686) \rightarrow \gamma\chi_{c0}$ (2.1%) and $\psi(3686) \rightarrow \gamma\chi_{c2}$ (2.1%) are taken from the PDG [4]. The uncertainties due to signal shape, damping factor and background are studied using a same method as the mass split and width measurement. The cross-contaminations between $\gamma\pi^+\pi^-$ and γK^+K^- events are studied via MC simulations, with input BFs updated by this measurement. The fluctuations due to BFs are taken as systematic uncertainties.

Table III summarizes all these sources and their contributions to BF measurements. Assuming all the sources are independent, the total systematic uncertainties are obtained by adding them in quadrature. The largest systematic uncertainty comes from the intermediate BFs, and all other sources contribute about 1.2%.

TABLE III. Sources of systematic uncertainties and their contributions (in %) to BF measurements.

Source	$\gamma\pi^+\pi^-$ γK^+K^-			
	χ_{c0}	χ_{c2}	χ_{c0}	χ_{c2}
$N_{\text{tot}}[\psi(2S)]$	0.7	0.7	0.7	0.7
Tracking	0.1	0.1	0.2	0.1
Photon	0.5	0.5	0.5	0.5
Polynomial background	0.6	0.2	0.1	0.1
Number of $(\gamma)\mu^+\mu^-$ background	0.1	0.4	0.1	0.1
Shape of $(\gamma)\mu^+\mu^-$ background	0.2	0.1	0.1	0.1
Cross contamination	0.1
Damping factor	0.1	0.2	0.1	0.1
Signal shape	0.1	0.2	0.1	0.1
Angular distribution	...	0.1
4C kinematic fit	0.3	0.2	0.7	0.8
Sum	1.2	1.1	1.2	1.2
Intermediate BF	2.1	2.1	2.1	2.1
Total	2.4	2.4	2.3	2.4

In summary, a precise measurement of the χ_{c0} resonance parameters and the $\chi_{c0,c2} \rightarrow \pi^+\pi^-/K^+K^-$ decay BFs is performed at BESIII by analyzing $\psi(3686)$ data events. The mass split between χ_{c2} and χ_{c0} is measured to be $\Delta M_{20} = (140.50 \pm 0.07 \pm 0.06) \text{ MeV}/c^2$. Taking the χ_{c2} world average mass as input, the χ_{c0} mass is determined to be $M(\chi_{c0}) =$

$(3415.67 \pm 0.07 \pm 0.06 \pm 0.07) \text{ MeV}/c^2$, where the first uncertainty is statistical, the second systematic, and the third from χ_{c2} mass uncertainty. This is the most precise χ_{c0} mass measurement to date. It is a bit higher ($1.46 \pm 0.49 \text{ MeV}/c^2$) than the BES measurement [8], while agrees well with the E835 measurement [9]. Our measurement improves the precision of χ_{c0} mass over previous individual measurements by a factor of four [8, 9]. The full width of χ_{c0} is measured to be $\Gamma(\chi_{c0}) = (12.44 \pm 0.12 \pm 0.12) \text{ MeV}$. It agrees with the BES measurement quite well within 1σ [8] and improves the precision by an order of magnitude. These measurements have a big impact on our knowledge about the χ_{c0} resonance parameters [4], and are expected to play a crucial role in our understanding of the strong force governing the $c\bar{c}$ system [39, 44].

The decay BFs are measured to be

$$\begin{aligned} \mathcal{B}(\chi_{c0} \rightarrow K^+ K^-) &= (6.36 \pm 0.02 \pm 0.08 \pm 0.13) \times 10^{-3}, \\ \mathcal{B}(\chi_{c0} \rightarrow \pi^+ \pi^-) &= (6.06 \pm 0.02 \pm 0.07 \pm 0.13) \times 10^{-3}, \\ \mathcal{B}(\chi_{c2} \rightarrow K^+ K^-) &= (1.22 \pm 0.01 \pm 0.02 \pm 0.03) \times 10^{-3}, \\ \mathcal{B}(\chi_{c2} \rightarrow \pi^+ \pi^-) &= (1.61 \pm 0.01 \pm 0.02 \pm 0.04) \times 10^{-3}, \end{aligned}$$

where the first uncertainties are statistical, the second systematic, and the third come from $\mathcal{B}[\psi(3686) \rightarrow \gamma\chi_{c0,c2}]$ [4]. These measurements agree with the CLEO-c result within 1σ [45], and improve the precision by more than threefold. Interestingly, the ratio of BFs $\frac{\mathcal{B}(\chi_{c0} \rightarrow K^+ K^-)}{\mathcal{B}(\chi_{c0} \rightarrow \pi^+ \pi^-)}$ is close to one, implies no significant ‘Chiral Suppression’ observed for a 0^{++} system [20, 21], which is different from the case of the glueball candidate $f_0(1710)$ [18, 19] and provides important input for the study of glueballs.

The BESIII Collaboration thanks the staff of BEPCII and the IHEP computing center for their strong support. We are also grateful to Prof. Chen Ying for the inspiring discussion on glueballs. This work is supported in part by National Key R&D Program of China under Contracts Nos. 2020YFA0406300, 2020YFA0406400, 2023YFA1606000; National Natural Science Foundation of China (NSFC) under Contracts Nos. 11635010, 11735014, 11935015, 11935016, 11935018, 12025502, 12035009, 12035013, 12061131003, 12192260, 12192261, 12192262, 12192263, 12192264, 12192265, 12221005, 12225509, 12235017, 12361141819; the Chinese Academy of Sciences (CAS) Large-Scale Scientific Facility Program; the CAS Center for Excellence in Particle Physics (CCEPP); Joint Large-Scale Scientific Facility Funds of the NSFC and CAS under Contract No. U1832207; 100 Talents Program of CAS; Project No. ZR2022JQ02, ZR2024QA151 supported by Shandong Provincial Natural Science Foundation; supported by the China Postdoctoral Science Foundation under Grant No. 2023M742100; The Institute of Nuclear and Particle Physics (INPAC) and Shanghai Key Laboratory for Particle Physics and Cosmology; German Research Foundation DFG under Contracts Nos. FOR5327, GRK 2149; Istituto Nazionale di Fisica Nucleare, Italy; Knut and Alice Wallenberg Foundation under Con-

tracts Nos. 2021.0174, 2021.0299; Ministry of Development of Turkey under Contract No. DPT2006K-120470; National Research Foundation of Korea under Contract No. NRF-2022R1A2C1092335; National Science and Technology fund of Mongolia; National Science Research and Innovation Fund (NSRF) via the Program Management Unit for Human Resources & Institutional Development, Research and Innovation of Thailand under Contracts Nos. B16F640076, B50G670107; Polish National Science Centre under Contract No. 2019/35/O/ST2/02907; Swedish Research Council under Contract No. 2019.04595; The Swedish Foundation for International Cooperation in Research and Higher Education under Contract No. CH2018-7756; U. S. Department of Energy under Contract No. DE-FG02-05ER41374.

-
- [1] T. Appelquist, A. De Rújula, H. D. Politzer, and S. L. Glashow, *Phys. Rev. Lett.* **34**, 365 (1975).
 - [2] E. Eichten, K. Gottfried, T. Kinoshita, J. B. Kogut, K. D. Lane, and T.-M. Yan, *Phys. Rev. Lett.* **34**, 369 (1975), [Erratum: *Phys.Rev.Lett.* 36, 1276 (1976)].
 - [3] E. Eichten, K. Gottfried, T. Kinoshita, K. D. Lane, and T. M. Yan, *Phys. Rev. D* **17**, 3090 (1978).
 - [4] S. Navas *et al.* (Particle Data Group), *Phys. Rev. D* **110**, 030001 (2024).
 - [5] T. A. Armstrong *et al.* (E760), *Nucl. Phys. B* **373**, 35 (1992).
 - [6] M. Andreotti *et al.*, *Nucl. Phys. B* **717**, 34 (2005), [arXiv:hep-ex/0503022](#).
 - [7] R. Aaij *et al.* (LHCb), *Phys. Rev. Lett.* **119**, 221801 (2017), [arXiv:1709.04247 \[hep-ex\]](#).
 - [8] M. Ablikim *et al.* (BES), *Phys. Rev. D* **71**, 092002 (2005), [arXiv:hep-ex/0502031](#).
 - [9] S. Bagnasco *et al.* (Fermilab E835), *Phys. Lett. B* **533**, 237 (2002).
 - [10] C. J. Morningstar and M. J. Peardon, *Phys. Rev. D* **60**, 034509 (1999), [arXiv:hep-lat/9901004](#).
 - [11] E. Gregory, A. Irving, B. Lucini, C. McNeile, A. Rago, C. Richards, and E. Rinaldi, *JHEP* **10**, 170 (2012), [arXiv:1208.1858 \[hep-lat\]](#).
 - [12] H. B. Meyer, *Glueball regge trajectories*, Other thesis (2004), [arXiv:hep-lat/0508002](#).
 - [13] S. J. Brodsky, A. S. Goldhaber, and J. Lee, *Phys. Rev. Lett.* **91**, 112001 (2003), [arXiv:hep-ph/0305269](#).
 - [14] E. Braaten and J. Lee, *Phys. Rev. D* **67**, 054007 (2003), [Erratum: *Phys.Rev.D* 72, 099901 (2005)], [arXiv:hep-ph/0211085](#).
 - [15] K.-Y. Liu, Z.-G. He, and K.-T. Chao, *Phys. Lett. B* **557**, 45 (2003), [arXiv:hep-ph/0211181](#).
 - [16] K. Abe *et al.* (Belle), *Phys. Rev. Lett.* **89**, 142001 (2002), [arXiv:hep-ex/0205104](#).
 - [17] H.-W. Huang and K.-T. Chao, *Phys. Rev. D* **54**, 6850 (1996), [Erratum: *Phys.Rev.D* 56, 1821 (1997)], [arXiv:hep-ph/9606220](#).
 - [18] M. Ablikim *et al.* (BES), *Phys. Lett. B* **603**, 138 (2004), [arXiv:hep-ex/0409007](#).
 - [19] M. Ablikim *et al.*, *Phys. Lett. B* **642**, 441 (2006), [arXiv:hep-ex/0603048](#).
 - [20] M. Chanowitz, *Phys. Rev. Lett.* **95**, 172001 (2005), [arXiv:hep-ph/0506125](#).
 - [21] K.-T. Chao, X.-G. He, and J.-P. Ma,

- Phys. Rev. Lett. **98**, 149103 (2007), arXiv:0704.1061 [hep-ph].
- [22] J. Bolz, P. Kroll, and G. A. Schuler, Phys. Lett. B **392**, 198 (1997), arXiv:hep-ph/9610265.
- [23] M. Ablikim *et al.* (BESIII), Chin. Phys. C **48**, 093001 (2024), arXiv:2403.06766 [hep-ex].
- [24] M. Ablikim *et al.* (BESIII), Nucl. Instrum. Meth. A **614**, 345 (2010), arXiv:0911.4960 [physics.ins-det].
- [25] C. Yu *et al.*, in *7th International Particle Accelerator Conference* (2016) p. TUYA01.
- [26] M. Ablikim *et al.* (BESIII), Chin. Phys. C **44**, 040001 (2020), arXiv:1912.05983 [hep-ex].
- [27] S. Agostinelli *et al.* (GEANT4), Nucl. Instrum. Meth. A **506**, 250 (2003).
- [28] S. Jadach, B. F. L. Ward, and Z. Was, Phys. Rev. D **63**, 113009 (2001).
- [29] S. Jadach, B. Ward, and Z. Was, Computer Physics Communications **130**, 260–325 (2000).
- [30] M. Ablikim *et al.* (BESIII), Phys. Rev. D **84**, 092006 (2011), arXiv:1110.1742 [hep-ex].
- [31] D. J. Lange, Nucl. Instrum. Meth. A **462**, 152 (2001).
- [32] R.-G. Ping, Chin. Phys. C **32**, 599 (2008).
- [33] J. C. Chen, G. S. Huang, X. R. Qi, D. H. Zhang, and Y. S. Zhu, Phys. Rev. D **62**, 034003 (2000).
- [34] R.-L. Yang, R.-G. Ping, and H. Chen, Chin. Phys. Lett. **31**, 061301 (2014).
- [35] E. Barberio, B. van Eijk, and Z. Was, Computer Physics Communications **66**, 115 (1991).
- [36] G. Balossini, C. Bignamini, C. M. C. Calame, G. Montagna, O. Nicrosini, and F. Piccinini, Phys. Lett. B **663**, 209 (2008), arXiv:0801.3360 [hep-ph].
- [37] M. Ablikim *et al.* (BESIII), Chin. Phys. C **42**, 023001 (2018), arXiv:1709.03653 [hep-ex].
- [38] N. Brambilla *et al.*, Eur. Phys. J. C **71**, 1534 (2011), arXiv:1010.5827 [hep-ph].
- [39] T. Barnes, S. Godfrey, and E. S. Swanson, Phys. Rev. D **72**, 054026 (2005), arXiv:hep-ph/0505002.
- [40] V. V. Anashin *et al.*, Int. J. Mod. Phys. Conf. Ser. **02**, 188 (2011), arXiv:1012.1694 [hep-ex].
- [41] R. E. Mitchell *et al.* (CLEO), Phys. Rev. Lett. **102**, 011801 (2009), [Erratum: Phys.Rev.Lett. 106, 159903 (2011)], arXiv:0805.0252 [hep-ex].
- [42] R. Barlow, in *PHYSTAT (2005): Statistical Problems in Particle Physics, Astrophysics and Cosmology* (2004) pp. 56–59, arXiv:physics/0406120.
- [43] M. Ablikim *et al.* (BESIII), Phys. Rev. D **87**, 012002 (2013), arXiv:1208.4805 [hep-ex].
- [44] W. Lucha, F. F. Schoberl, and D. Gromes, Phys. Rept. **200**, 127 (1991).
- [45] D. M. Asner *et al.* (CLEO), Phys. Rev. D **79**, 072007 (2009), arXiv:0811.0586 [hep-ex].